13th International Brick and
Block Masonry Conference
Amsterdam, July 4-7, 2004

Flexural behavior of representative panels of prefabricated reinforced masonry shells

J.T. Oliveira[1], J.O. Barros[2], P.B. Lourenço[3], E. Bonaldo[4],

Abstract

Reinforced masonry shells were widely used in the past by Eladio Dieste. In order to develop a modern competitive technology for the building industry, a prefabrication process to build such structures has been investigated and the necessary tests to characterize the constitutive materials have been carried out. Here, an experimental program of bending tests in reinforced masonry panels is detailed. The panels were made of a concrete topping layer reinforced with welded wire mesh, ceramic facing bricks and reinforced concrete joints. The panels were tested for both positive and negative bending moments. A numerical approach was developed to predict the deformational and the load bearing capacity of such structures.

Key Words

Reinforced masonry, shell, flexural testing, prefabrication.

1 Introduction

The research presented here is part of a European project based on shell buildings executed by Eladio Dieste, Junta de Andalucia (1996). This Uruguayan engineer designed a significant number of curved masonry shells for roofs and walls. Such buildings were built mainly in South America since 1950. Dieste's shells were composed of ceramic bricks in stack bond, so that orthogonal reinforcement could be introduced. The reinforced joints and the topping were made of mortar. The technology was low-cost, aesthetically appealing and structurally efficient, as it allows taking advantage of the properties of each material component.

One of the advantages of the system adopted by Dieste was that the same mould could be used several times in a repetitive pattern. However, in order to become an attractive building system for the today developed countries, a prefabricated process

[1] PhD student, University of Minho, 4800-058 Guimarães, Portugal, juliana@civil.uminho.pt
[2] Assistant Professor, University of Minho, barros@civil.uminho.pt
[3] Associate Professor, University of Minho, pbl@civil.uminho.pt
[4] PhD student, University of Minho, bona@civil.uminho.pt

has to be implemented. Nowadays, fastness, moderate workmanship demands and an economical molding system are key desired characteristics of the building industry. Thus, the aim of the current project is to contribute for the European construction sector by providing a cheap, efficient, ecological, secure, simple and industrialized mean to construct thin shell roofs with high quality. The developed system has to be attractive from the technical and economical points of view.

One possible strategy for the development of the system is to adopt prefabrication. The prefabricated model is composed by a layer of ceramic bricks, bonded by concrete joints of 25 mm thickness and covered by a concrete layer of 30 mm thickness. The concrete joints form a grid reinforced with steel bars. The concrete layer is reinforced with welded wire mesh positioned near the brick-concrete layer interface. To test the feasibility of the technique, a shell was built at the laboratory of Minho University, following a catenary directrix (see Figure 1a), according Oliveira et al (2003a).

Assessing the mechanical behavior of representative elements of the entire shell will help to understand its structural behavior. For this purpose, four point bending tests were carried out according to EN 1052-2 (2000). The building process of the specimens followed the same procedures applied in the entire shell (Figure 1b). Here, the obtained experimental results are presented and discussed. A simple numerical model was also developed to simulate the behavior of this type of elements.

(a) (b)

Figure 1 Model of the entire shell (a); detail of the specimen to be tested before the concrete casting (b)

2 Characterization of the specimens and test set-up

2.1 Materials

The adopted concrete was made with 300 Kg/m^3 of cement 42.5 R, 279 Kg/m^3 of sand 0.6-5 mm, 655 Kg/m^3 of sand 0.3-0.6 mm and 806 Kg/m^3 of gravel 5-10 mm. Rebuilt®1000 superplasticizer was used in a content of 2.5% of the cement quantity. The water/cement ratio was 0.55. Due to the fact that masonry joints were narrow, the joints were reinforced and the shell was curved, concrete was designed to fill the joints without segregation or slipping. The designed concrete had a slump of 210 mm.

The concrete strength is given in Table 1 for the different panel series, where f_{cm} is the average compression strength and $f_{fctm,fl}$ is the average flexural tensile strength. The average uniaxial tensile strength, $f_{fctm,ax}$, was estimated according to CEB-FIP (1993). Each value of Table 1 is the average of, at least, three tests.

The brick average dimensions were 215 mm length, 100 mm width and 65 mm height (see Figure 2), with square holes of 25 mm edge. Polystyrene pieces were introduced in the ends of the brick holes to avoid excessive concrete penetration. The compressive strength in X and Y directions were 71.8 N/mm^2 and 31.8 N/mm^2, respectively, according Lourenço et al (2004). The compressive tests were carried out according to EN 772-1 (2000). The values of tensile strength for the X and Y directions were 3.50 N/mm^2 and 1.76 N/mm^2, respectively, according to Almeida et al (2002).

Table 1 Tested concrete properties (bending and compression tests)

Specimens	$f_{fctm,fl}$ (N/mm^2)	$f_{fctm,ax}$ (N/mm^2)	f_{cm} (N/mm^2)
Average FLs-A	3.98	1.59	35.60
Average FLs-B	4.24	1.69	42.19
Average FLIs-A	5.04	2.02	36.75
Average FLIs-B	4.46	1.78	38.39

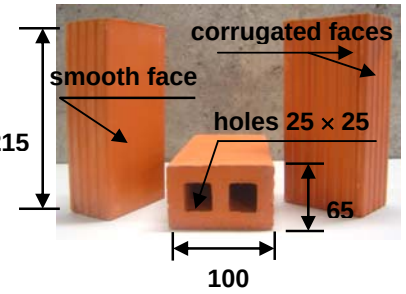

Figure 2 Brick dimensions (mm)

The reinforcement in the parallel (longitudinal reinforcement) and in the orthogonal (transversal reinforcement) direction of the brick holes was made of steel bars of 8 mm and 6 mm diameter, respectively. In the concrete topping, immediately above the brick units, a welded wire mesh of bars of 3 mm diameter, spaced at 75 mm, was placed. The bars were tested according to EN 10002-1 (1990). Table 2 includes the main data obtained from these tests. Figure 3 illustrates the steel bars distribution in the panels.

Table 2 Characterization of steel bars (strength values in N/mm^2)

	Steel bars				Wire mesh	
	ϕ 8mm	C.V.%	ϕ 6mm	C.V.%	ϕ 3mm	C.V.%
Yield stress at 0.2%	524	4.5	668	8.7	545	4.69
Tensile strength	614	2.5	698	9.5	824	5.92

2.2 Specimens (panels)

The panels were divided in four series of four panels each:

Series FL-A: panels tested with the concrete topping turned upwards and the line loads applied directly on concrete topping, in the direction of the brick holes (Figure 3a);

Series FL-B: panels tested with the concrete topping turned upwards and the line loads applied directly on concrete topping, perpendicular to the direction of the brick holes (Figure 3b);

Series FLI-A: panels similar to the series FL-A, but tested with the concrete topping turned downwards;

Series FLI-B: panels similar to the series FL-B, but tested with the concrete topping turned downwards.

The dimensions of the panels of series FL-A were 975 mm of length, 455 mm of width and 95 mm of thickness. For panels of series FL-B these dimensions were, respectively, 935 mm, 375 mm and 95 mm. The differences in the in-plane dimensions of panels of series FL-A and FL-B are due to the brick in-plane distinct dimensions, resulting the two possible brick arrangements schematically represented in Figure 3. The force was applied by two line loads in the panel's width, at a distance of 187.5 mm from the middle of the panel. The external supports were placed at a distance of 437.5 mm (FL-A) and 420 mm (FL-B) from the panel center (see Figure 3).

2.3 Test set-up

The design of concrete/masonry based shell structures can be conditioned by the flexural strength. Moreover, due to brick shape, bond and reinforcement arrangement, the stiffness and the strength in the shell orthotropic directions can be distinct.

Therefore, assessing the bending behavior in the two shell orthotropic directions is a key issue. Figure 4 shows the test set up of the panels of series FL-A and FL-B. The panels of series FLI-A and FLI-B have the same test set up of series FL-A and FL-B, respectively, but those panels were tested with the concrete layer downwards.

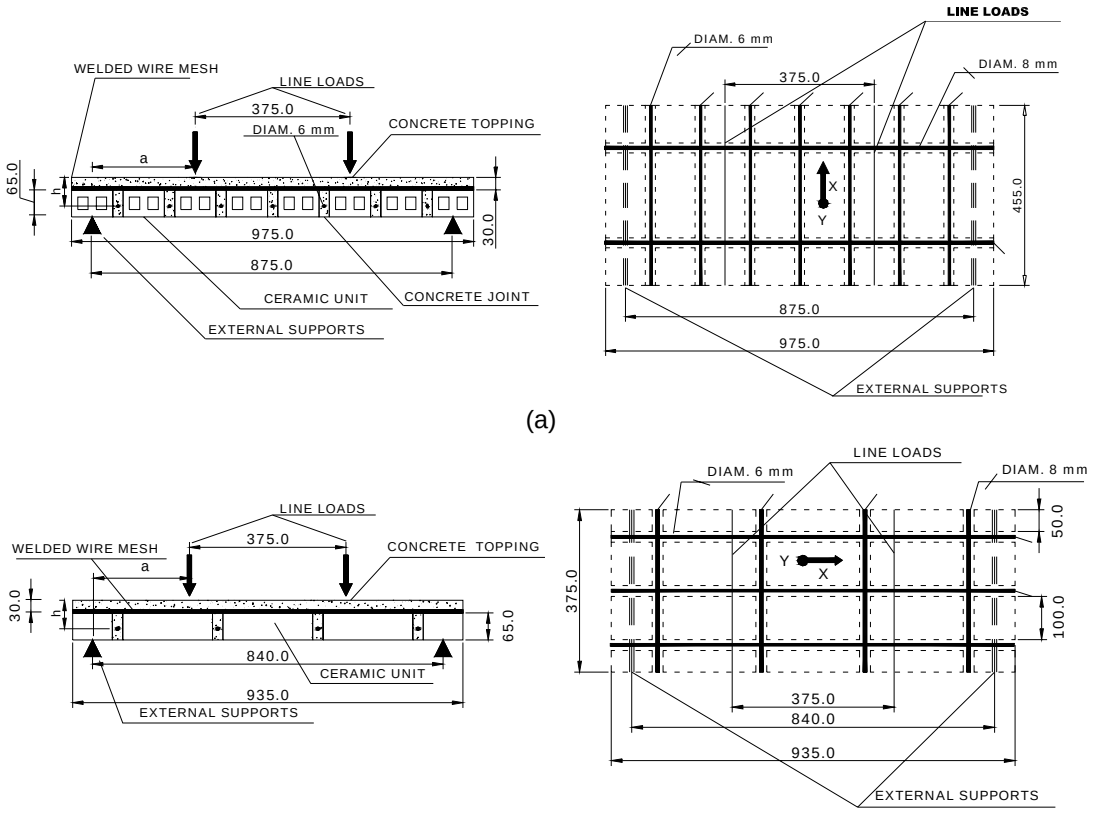

Figure 3 Panels of series FL-A(a) and FL-B (b)

(a) (b)

Figure 4 Test set up for panels of series FL-A(a) and series FL-B(b)

The applied load was measured from a load cell of 200 kN bearing capacity, 0.1% tolerance and sensitivity, attached to a servo-hydraulic actuator of 500 kN maximum bearing capacity. In selected panels, the strain variation of some steel bars that reinforce the concrete joints was registered using strain gauges. The tests were carried out under displacement control, at a displacement rate of 0.015 mm/s, using the displacement transducer placed at panel mid span for this purpose, see Oliveira et al (2003b) for details.

3 Test results

3.1 Series FL-A

In this series a large number of thin cracks occurred in the constant bending zone (between the line-loads), mainly at the brick-concrete joint interfaces. In some tests, bars of the wire mesh crossing the failure crack were ruptured and holes of the brick elements were intersected by the failure crack (see Figure 5). Crushing of the concrete topping layer was observed at the structural softening phase. Figure 6 represents the relationship between the total load and the panel central deflection for the panels of series FL-A. The shape of these curves are similar to the reinforced concrete elements failed by bending, i.e., having ductile failure mode. Figure 7 shows a representative strain variation in the longitudinal steel bars. The position of the strain gauges (SG) is indicated in Figure 8. After steel yielding (at about 2620 μstrains, which is in agreement with the results obtained in the bar tensile tests), a sudden increase of strain occurred, followed by a continuous decrease of strain with the load increment. This strain decrease in the final phase of the test was caused by reinforcement-concrete sliding, indicating that there were some difficulties in assuring good bond properties for the bars reinforcing the concrete joints of 25 mm width.

Figure 5 Typical failure mode of panel of series FL-A

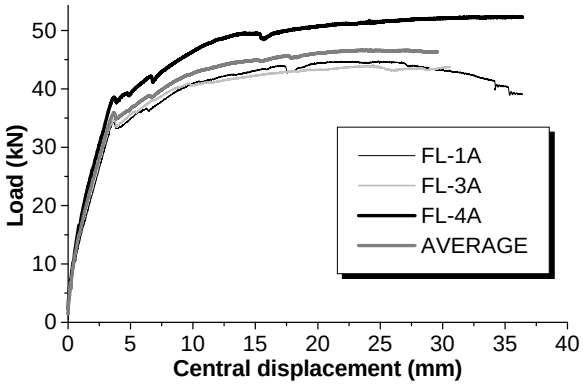

Figure 6 Load-deflection of panels of series FL-A

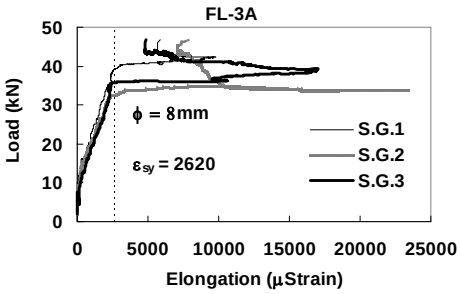

Figure 7 Relationship between the load and the strains at steel bars

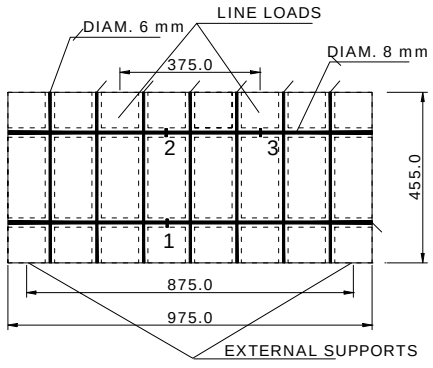

Figure 8 Positions of the strain gauges (SG)

3.2 Series FL-B

In general, failure crack of panel of series FL-B occurred near the panel mid-span, crossing the brick elements (see Figure 9). In these panels the cracks were not initiated at concrete joint-brick interfaces since the brick holes were aligned in the longitudinal

direction and part of the concrete in the transversal joints has penetrated into the brick holes. This resulted in some interlocking between bricks and concrete joints, inhibiting the crack propagation at these interfaces. The load-deflection relationship of series FL-B is depicted in Figure 10.

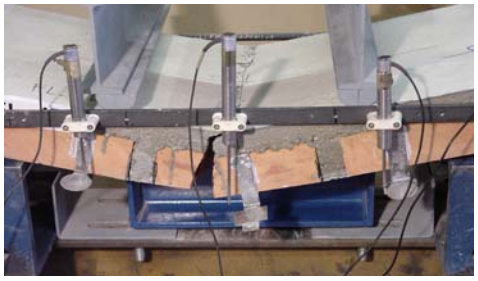

Figure 9 Typical failure mode of panel of series FL-B

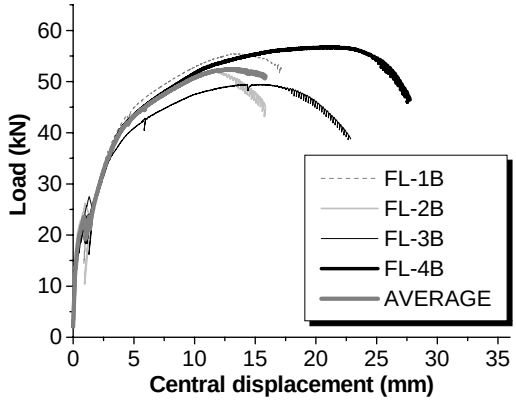

Figure 10 Load-deflection of panels of series FL-B

3.3 Series FLI-A

In general, after cracking the concrete layer, the cracks progressed through the brick holes (see Figure 11), which was accompanied by a significant reduction of the panel stiffness (see Figure 12). Due to insufficient longitudinal reinforcement for assuring stabilized cracking, a sudden load drop occurred just after cracking the concrete layer. The peak load coincided with the rupture of some wires of the wire mesh, which was followed by abrupt load decay. For deflections above 10 mm, the panels had a quasi-constant residual load bearing capacity.

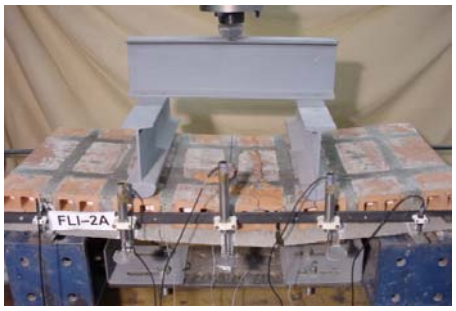

Figure 11 Typical failure mode of panel of series FLI-A

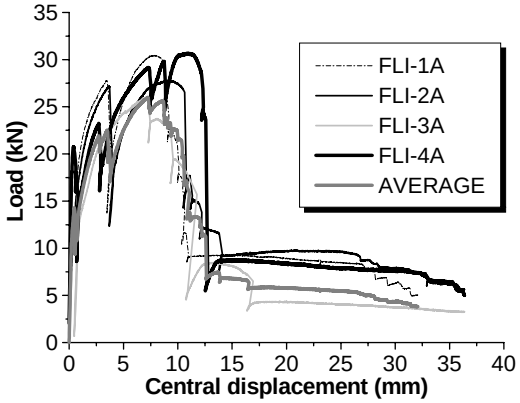

Figure 12 Load-deflection of panels of series FLI-A

3.4 Series FLI-B

The failure modes (see Figure 13), the crack patterns and the panel deflection of series FLI-B were similar to those of series FLI-A. Figure 14 includes the load-central deflection relationship of the panels of this series. In a first phase, the panels showed a quasi-elastic response. Afterwards, unloading-reloading cycles occurred due to the formation of macro-cracks and activation of the wire mesh.

The average of the force-central deflection relationship of each series of panels is represented in Figure 15. Series FLI-A and FLI-B had similar behavior, showing that the orthotropic arrangement of bricks and bars reinforcement have marginal influence when the loading induces, mainly, compression stresses in these elements. However,

in series FL-A and FL-B the aforementioned orthotropic arrangements had influence, mainly, in the maximum load bearing capacity and stiffness of the panels. In fact, despite FL-B has lower longitudinal reinforcement ratio than FL-A series (A_s = 84.8 mm^2 in FL-B and A_s = 100.5 mm^2 in series FL-A), series FL-B had larger load bearing capacity and stiffness than FL-A. The larger load bearing capacity of the former series can be justified by the highest values of the yield and ultimate stress of the longitudinal ϕ6mm bars of the panels of this series. The larger number of concrete ribs (joints) in the longitudinal direction of panel series FL-B can justify the larger stiffness of these panels (see Figure 3). Moreover, in series FL-B, concrete of the transversal joints has filled the ends of the brick holes, providing an interlock between bricks and transversal concrete joints, while in series FL-A the transversal concrete joints were bonded to the smooth brick surfaces.

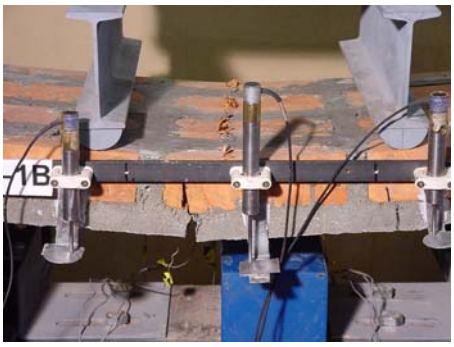

Figure 13 Typical failure mode of panel of series FLI-B

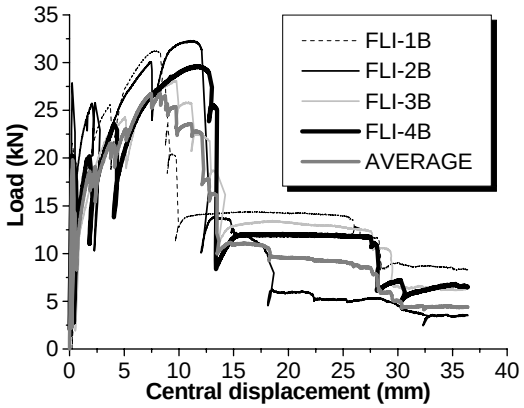

Figure 14 Load-deflection of panels of series FLI-B

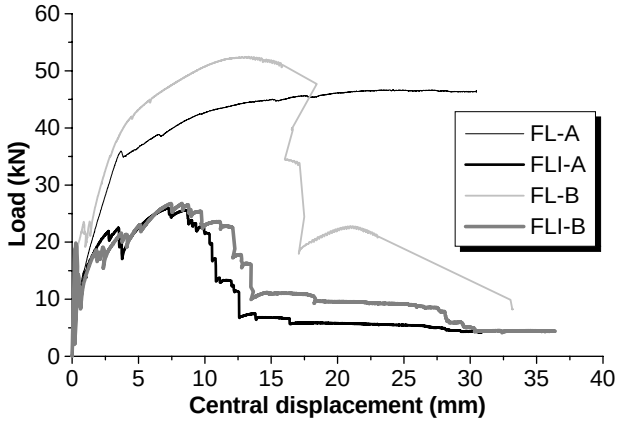

Figure 15 Relationship between the average force and the mid-span deflection for all the series

4 Numerical simulation

Previous works (Barros and Sena-Cruz 2001, Barros et al 2004) have shown that, using a cross-section layered model that takes into account the constitutive laws of the intervening materials, the kinematic and the equilibrium conditions, the deformational behavior of structural elements failing in bending can be predicted from the moment-curvature relation, M-χ, of the representative sections, using the algorithm described in Figure 16.

Due to lack of space, only two of the tested panels (FL-3A and FLI-3A) are simulated to assess the performance of the model developed, using Euler-Bernoulli two node beam elements. Due to the observed failure modes, two cross sections were assumed as

being representative of the panel structural behavior: one at the concrete joint-brick interface, and the other crossing the brick units. Figure 17 shows the representative cross sections of the panel FL-3A. Panel FLI-4A has identical cross sections, but the concrete layer is turned downwards. The cross sections were discretized in layers of 1 mm thick. The data used in the numerical simulation is in Table 3. Due to shell manufacture characteristics, concrete applied in the shell has considerably different properties from concrete evaluated in cylinder and prismatic specimens. In the shell manufacture, the concrete was cast without any compaction, resulting a concrete with high percentage of voids and, consequently, of low compacity and stiffness. To simulate a premature microcracking of the concrete layer, a bilinear diagram was used to model the pre-peak tensile strength behavior. The concrete properties indicated in Table 4 reflect these conditions. The post-cracking behavior of the concrete and bricks was simulated by a trilinear softening diagram, defined by the fracture parameters of these materials (Barros et al 2004). Tension stiffening was included in a trilinear post-cracking stress-strain diagram for concrete influenced by reinforcing bars.

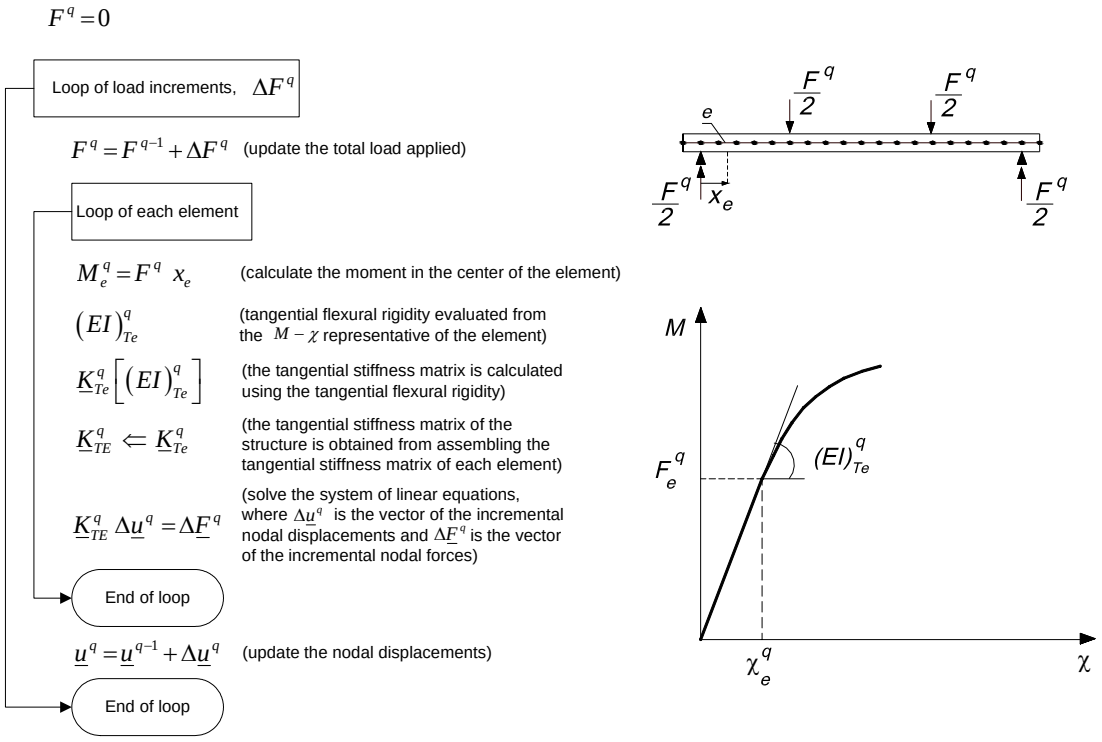

Figure 16 Numerical approach to simulate the deformational behavior of structural elements failing in bending.

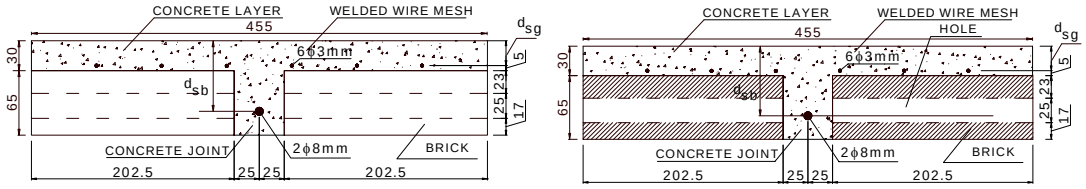

S1 - Concrete joint-brick interface *S2 - Crossing brick unites*

Figure 17 Representative cross sections of the panel FL-3A

As Figure 18 shows that, the simple numerical approach developed fits well the observed experimental load-central deflection of the tested panels.

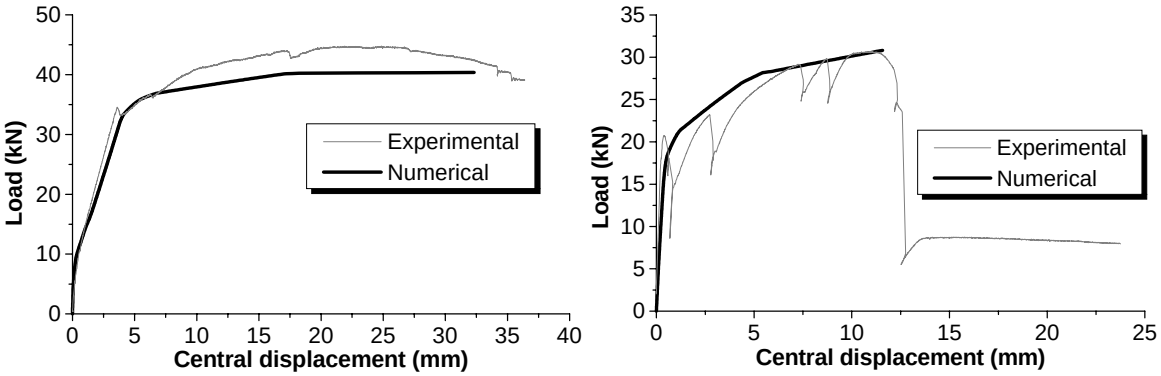

Figure 18 Experimental versus numerical load-central deflection of panel: FL-3A (a); FLI-4A (b)

Table 3 Material properties in the numerical simulation

Panel		FL-3A	FLI-4A
Concrete	f_{cm} (N/mm^2)	37.90	36.37
	f_{ctm} (N/mm^2)	2.90	2.10
	E_c (N/mm^2)	33500	29700
Concrete joint-brick interface	f_t (N/mm^2)	0.60	
	E (N/mm^2)	10000	
Brick	f_c (N/mm^2)	32.80	
	f_t (N/mm^2)	2.00	
	E (N/mm^2)	10000	
Steel Rebar (ϕ 8mm)	f_y (N/mm^2)	524	
	f_s (N/mm^2)	614	
Steel welded mesh	f_y (N/mm^2)	545	
	f_s (N/mm^2)	824	

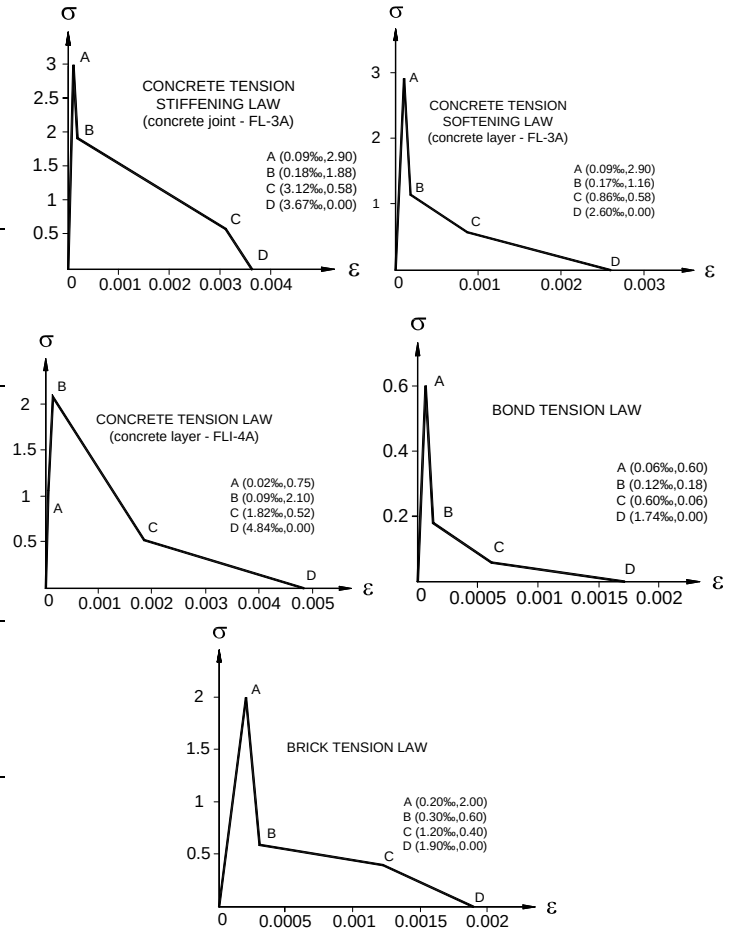

5 Conclusions

To assess the flexural behavior of reinforced masonry shells submitted to downwards and upwards loadings, four point bending tests on representative panels were carried out. In the experimental program the material orthotropy resulting from the possible distinct arrangements of bricks and reinforcing bars was taken into account. In panels with the concrete layer at top surface, the highest stiffness and maximum load bearing

capacity occurred in panels with the higher number of longitudinal concrete joints and steel bars of larger yield and ultimate stress. In the series of these panels, cracks were initiated at the interfaces between bricks and transversal concrete joints. In panels with the brick holes in the panel longitudinal direction, some interlock due to concrete penetration into the extremities of these holes has assured higher resistance to crack propagation in these interfaces, resulting cracks crossing the bricks. Both series of this type of panels failed in a bending ductile mode. As concrete was applied without external compacting energy, it had low compacity, which resulted in sliding between reinforcing bars and surrounding concrete. The panels with the concrete layer at panel bottom surface had a load bearing capacity of about half of the one of their counterpart panels with the concrete layer at panel top surface. In comparison with these last panels, the former ones showed a more fragile failure mode.

A cross section layer model was used to determine the moment-curvature relationship, M-χ, of the representative sections of the tested panels. The M-χ was used to evaluate the tangential flexural stiffness, $(EI)_T$ during the panel loading process. The tangential stiffness matrix of the panel was evaluated from the $(EI)_T$ of each element discretizing the panel, and using the framework of the matrix displacement method. This simple numerical strategy was able to predict, with enough accuracy, the force-deflection relationship registered experimentally.

Acknowledgements

The study presented here is partly sponsored by contract part of the research program “Industrialized Solutions for Construction of Masonry Shell Roofs”, supported by the European Commission. Acknowledgements are also due to SECIL, Bezerras’ Quarry and Bettor MBT Portugal. The first and last authors acknowledge the PhD grant supported by the Portuguese Science and Technology Foundation (FCT).

References

Almeida J.C., Lourenço P.B., Barros, J.A. Characterization of brick and brick–mortar interface under uniaxial tension. In: Santos FA *et al.*, editors. Proceedings of 7th Int. Seminar on Structural Masonry, Brazil: CEFET-MG, 2002. p. 67-76.

Barros, J.A.O., Sena-Cruz, J.M. “Fracture energy of steel fibre reinforced concrete“, Journal of Mechanics of Composite Materials and Structures, Vol. 8, No. 1, Jan.-Mar. 2001, pp.29-45.

Barros, J.A.O., Cunha, V.M.C.F., Ribeiro, A.F., Antunes, J.A.B.; “Post-Cracking Behaviour of Steel Fibre Reinforced Concrete" accepted to be published in the RILEM Materials and Structures Journal in 2004.

CEB-FIP Model Code 1990 *Comite Euro-International du Beton*, Bulletin d’Information nº 213/214, Ed. Thomas Telford, 1993.

CEN. European norm for methods of test for masonry units – Part 1: Determination of compressive strength. EN 772-1, 2000.

CEN. EN 10002-1 – Tensile Testing, Part 1: method of test, 1990.

CEN. EN 1052-2, European norm for methods of test for masonry – Part 2: Determination of flexural strength, 2000.

Junta de Andalucía, Eladio Dieste 1943-1996. Montevideo, November, 1996.

Lourenço, P.B., Barros, J.O., Oliveira, J.T., Shear testing of stack bonded masonry, Construction and Building Materials, 18, 2004, pp.125-132.

Oliveira J. T., Barros J.O, Lourenço P.B, Bonaldo E. Contribution for a full prefabrication approach of masonry shells. Report nº 03-DEC/E-05. Universidade do Minho, Portugal, 2003a. pp. 17.

Oliveira J. T., Barros J.O, Lourenço P.B, Bonaldo E. Flexural behavior of reinforced masonry panels. Report nº 03-DEC/E-12. Universidade do Minho, Portugal, 2003b. pp. 76.